An air-charged Stirling-cycle refrigerator with novel isothermalisers

An air-charged Stirling-cycle refrigerator with novel isothermalisers

***Jafar* M. Daoud**[1, *] and ***Daniel* Friedrich**[2]

[1]College of Engineering and Technology, Palestine Technical University-Kadoorie (PTUK), Palestine
[2]Institute for Energy Systems, School of Engineering, University of Edinburgh, EH9 3DW (Scotland)
[*]Corresponding author: j.daoud@ptuk.edu.ps

Abstract

While the Stirling cycle is a simple thermodynamic cycle, energy dense machines are expensive and complex due to the complicated heat exchangers. Heat exchangers are essential to increase the heat transfer but they increase the dead volume, cost and pumping losses. In this contribution, a simple and novel isothermaliser is proposed that improves the cooling power density of the Stirling-cycle refrigerator without adding to the dead volume. Simulations based on the second order polytropic model show that the cooling power and efficiency can be enhanced and the regenerator losses can be significantly reduced. The novel isothermaliser leads to better performance than the conventional Stirling refrigerator at temperatures of 27/7^{o} C achieving higher cooling density per swept volume of 2.5 folds. The increased power density enables the Stirling refrigerator to compete with the vapour compression cycle in both high-lift and near-ambient refrigeration.

Keywords: Stirling cycle, Near-ambient refrigeration, Isothermalisers.

Introduction

The Vapour compression cycle (VCC) is the most widely used refrigeration technology for the near ambient market because it has the highest COP among other cooling technologies [1][2][3]. However, the refrigerants used with the VCC are often non-environmental-friendly since they are considered toxic, flammable, have ozone depletion potency and can participate in global warming. An alternative is the Stirling cycle refrigerator which is simple, has safe and quiet operation, low maintenance requirement, high theoretical efficiency and uses benign gases. It is a good competitor to the VCC in high-lift refrigeration where it achieves better performance and is also cheaper. The performance reaches a peak for an absolute temperature ratio around two in only one stage of refrigeration [4] for which, the performance of the VCC deteriorates [5]. Although, the ideal Stirling cycle has higher COP than the inverse Rankine cycle [66] the Stirling cycle refrigerator has not been successful at low lift refrigeration. The practical Stirling refrigerator lags behind the VCC as its cooling capacity decreases with the COP [6]. The Stirling refrigerator can achieve the efficiency of the VCC at a given cooling load but it is not cost-competitive [7]. Walker et al. doubted that the Stirling cycle refrigerator can compete economically with the VCC refrigerator due to the large number of VCC units produced every year [8]. In contrast, only few Stirling refrigerators are available for limited applications due to their initial and running costs [9]. Berchowitz et al. developed a free piston refrigerator for domestic refrigeration [10] and portable coolers [11][12]. The refrigerator showed a total efficiency of 35% of Carnot efficiency, which is

[*]Corresponding author: j.daoud@ptuk.edu.ps

comparable to the VCC. The portable coolers are powered by a PV collector and have a COP of three while the Carnot COP is 9.1. Oguz and Ozkadi [13] tested the free piston Stirling refrigerator for domestic refrigeration and showed that the main challenge is using complicated heat exchangers. Thus, the Stirling cooler can be an alternative to the VCC if the cost and complexity of the heat exchangers is reduced while maintaining the performance.

The Stirling cycle is an external combustion cycle that needs to convey heat from the working gas to the heat source via heat exchangers. Efficient heat exchangers enhance the heat transfer to achieve high refrigeration rates but at the cost of increasing the complexity, dead volume, power losses and machine price [14][15]. The expansion and compression volumes are usually unheated and their operation tends to be adiabatic. Walker [16] reported that the actual COP ratio of the Stirling cycle refrigerator due to the adiabatic cycles has a maximum absolute temperature between 100-150K. Bauwens [4] showed numerically that the adiabatic losses play the major role in decreasing the COP ratio at low-lift refrigeration which is hard to improve without decreasing the refrigeration load. Carlson et al. [17] showed the adiabatic cycle efficiency at low-lift refrigeration tends to less than 50% of the isothermal efficiency and the cooling power decreases for non-ideal adiabatic processes. Walker [16] suggested isothermalising the freezers and coolers as they are designed to maximise the heat transfer. Orlowska [18] suggested adding the isothermaliser in particular to the compression space to improve the COP of a refrigerator. The isothermalisers differ from the external heat exchangers in that they are within the expansion and compression spaces and not in series with them. Accordingly, the expansion and compression processes are neither isothermal nor adiabatic, but polytropic. The polytropic cycle cannot achieve Carnot efficiency for both the Stirling power cycle and heat pump. For example, at the maximum power point, the engine efficiency cannot exceed the Curzon and Ahlborn limit [19] where the working gas temperature is not equal to source temperature. The temperature difference causes irreversibility but helps to increase the heat transfer and hence reduce the gas friction losses. On the other hand, Stirling cycle refrigerators have no maximum cooling power due to the monotonic response of the cooling power to the COP [20][21][22]. Leff and Teeters [23] attributed the monotonic response to possible unbounded temperatures in contrast to the engine that works between two limits. Thus, the Carnot efficiency can be ideally approached when the cooling power is zero and the COP approaches zero for the highest cooling power. However, due to the potential Stirling refrigerator losses, the maximum COP and maximum cooling power might be reached [5][24].

Daoud and Friedrich [25] proposed a novel machine geometry for conveying the heat by the cylinder wall instead of only the end plates. Thus, the Stirling cycle machine benefits from the whole surface of the cylinders and the temperature difference between gas and containing cylinders to transfer heat. In the Franchot arrangement, the conduction and shuttle losses, which are the major thermal loss in the Stirling cycle machine [5][26], are eliminated and the hysteresis losses can be ignored. In a later publication [27], the same authors innovated a new isothermaliser specially tailored for the direct heating and cooling purpose without any intermediate heat exchanger. The isothermalisers resulted in power improvements and reduction in volumetric flow rate. This work is an extension of our previous studies to Stirling refrigeration. It is a theoretical study based on the second-order polytropic model [25] which aims to obtain the performance curves of the isothermalised Franchot refrigerator by varying the phase angle, dead volume, cylinder diameters and the speed. Both, the bare cylinder and isothermalised cylinder are considered and the performance is evaluated for a speed range of 100-500 RPM.

Methodology

The proposed isothermaliser for the Franchot machine is shown in Figure 1. The Franchot machine was invented in 1885. It comprises two opposite alpha Stirling machines each with a distinct gas circuit but both share the same cylinders. The Franchot machine has no shuttle and axial heat conduction losses and the phase angle is controllable. The connecting rod can work as an adiabatic or isothermal fin causing the hydraulic diameter to decrease which increases the heat transfer and decreases the swept volume. The adiabatic fin refers to unheated or uncooled connecting rod whilst the isothermal fin refers to the rod having the same cylinder temperature. The isothermal fins have potential in air conditioning since the expansion cylinder can be directly exposed to the refrigerated space and the compression cylinder can be directly exposed to the ambient. The rod itself can be hollow to reduce its weight and heat capacity.

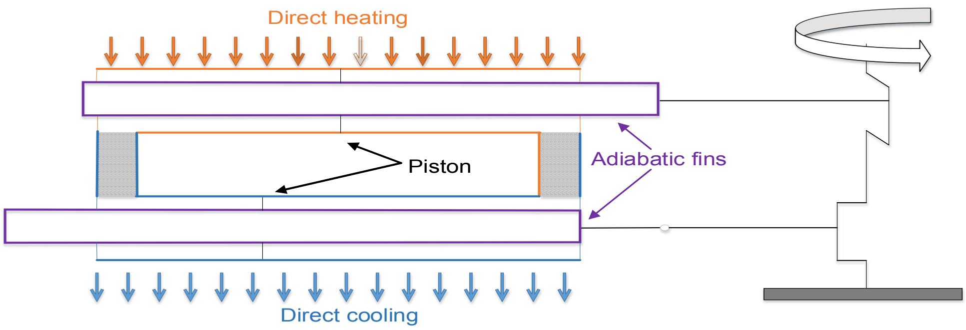

Figure 1: The proposed adiabatic fins inside the Franchot engine cylinders [27].

The heat addition and removal is calculated from Newton's law of cooling

$$\dot{Q}_e = hA\Delta T \quad (1)$$

The in cylinder heat transfer coefficient h is given by the correlations [28]

$$h_e = 0.042(D-d)^{-0.42}v^{0.58}p^{0.58}T^{-0.19}$$
$$h_c = 0.0236(D-d)^{-0.47}v^{0.53}p^{0.53}T^{-0.11} \quad (2)$$

where D and d are the diameters of the cylinder and rod, e and c are expansion and compression, respectively. According to the definition, the adiabatic fin, which is externally insulated, has a total heat flow equal to zero

$$\oint \dot{Q}_f = \oint hA_f\left(T_f - T_g\right) = 0 \quad (3)$$

where $h,\ A_f,\ T_f\ and\ T_g$ are the coefficient of heat transfer, fin area, fin temperature and gas temperature, respectively. The fluctuation in the connecting rod temperature is ignored because of the higher heat capacity of the stainless-steel rod in comparison to air. Hence, the fin temperature is supposed to be constant during a cycle. So, the average temperature of the adiabatic fin can be calculated as

$$T_f = \frac{\oint hA_fT_g}{\oint hA_f} \quad (4)$$

The Franchot engine consists of two alpha engines with two separate gas circuits. The pressure variation in each gas circuit is [25]

$$\dot{p} = \frac{-p\left(\frac{\dot{v}_e}{T_{re}} + \frac{\dot{v}_c}{T_{cr}}\right) + \frac{R}{c_p}\left(\frac{\dot{Q}_e}{T_{re}} + \frac{\dot{Q}_c}{T_{cr}}\right)}{\frac{v_e}{\gamma T_{re}} + \frac{V_r}{T_r} + \frac{v_c}{\gamma T_{cr}}} \quad 5$$

Regenerator end temperatures are calculated from

$$T_{rh} = \frac{-\oint i\dot{m}_e T_e}{\oint (1-i)\dot{m}_e}$$
$$T_{rk} = \frac{-\oint j\dot{m}_c T_c}{\oint (1-j)\dot{m}_c} \quad 6$$

where the parameters i and j are given by

$$i = \begin{cases} 1, & \dot{m}_e < 0 \\ 0, & \dot{m}_e \geq 0 \end{cases}$$
$$j = \begin{cases} 1, & \dot{m}_c < 0 \\ 0, & \dot{m}_c \geq 0 \end{cases} \quad 7$$

The average regenerator temperature is

$$T_r = \frac{T_{rh} - T_{rk}}{\ln\frac{T_{rh}}{T_{rk}}} \quad 8$$

The average engine power for the Franchot engine is calculated as

$$P = 2 * f \oint p(\dot{v}_e + \dot{v}_c) \quad 9$$

where f is the frequency. The pressure loss in the expansion and compression cylinders is calculated separately from the Zhao correlation for oscillatory turbulent pipe flow [29]:

$$\Delta p = -\frac{2\rho U_{max}^2 L}{X_m}\left(\frac{76.6}{\left(\frac{2D_h Re_{max}}{X_m}\right)^{1.2}} + 0.40624\right) \quad 10$$

The power loss in each cylinder is calculated from

$$P_p = \Delta p * \dot{v} \quad 11$$

where $\dot{v}$ is the volumetric flow rate of the working gas.

The polytropic model is applied to the alpha type engine with annular heat exchanger made by Karabulut [30]. The annular heat exchanger has the cylinder walls heated and the piston dome is of adiabatic fin type as shown in Figure 2.

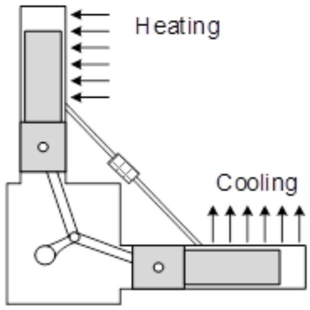

Figure 2: Karabulut alpha engine with annular heat exchangers: schematic diagram [30].

In the Karabulut engine, the heat exchanging area and volume are constant for the annulus and dynamic for the swept space. These conditions are replicated in our model for validation purpose. The technical specification of the engine is shown in Table 1.

Table 1: Technical specifications and operating conditions of the Karabulut engine [30].

Name	***value/unit***
Stroke length	*6 cm*
Bore diameter	*5.24 cm*
Piston dome diameter	*4.74 cm*
Hot annulus length	*13.5 cm*
Cold annulus length	*11 cm*
Connecting pipe length	*30 cm*
Connecting pipe diameter	*0.5cm*
Regenerator matrix	*Woven wire*
Wire diameter	*100 micron*
Regenerator porosity	*0.7*
Regenerator volume	*12 cm^3*
Out-of-Phase angle	*90^o*
Hot, cold temperatures	*1100^oC ,20^oC*
Working gas	*Air*
Average gas pressure	*1 bar, 2 bar*

To increase the accuracy of the model the reheat and pressure losses of the regenerator are considered. The effect of imperfect regeneration is considered by modifying the regenerator gas stream temperatures as [31][32]

$$\begin{aligned} T_{rho} &= T_{rk} + \varepsilon(T_{rh} - T_{rk}) \\ T_{rko} &= T_{rh} - \varepsilon(T_{rh} - T_{rk}) \end{aligned} \tag{12}$$

where, T_{rho}, T_{rko} *and* ε are the hot outlet gas temperature, cold outlet gas temperature and regenerator effectiveness, respectively. The enthalpy loss can be quantified by

$$\dot{Q} = c_p \dot{m} \Delta T(1 - \varepsilon) \tag{13}$$

The effectiveness is calculated according to Tanaka [33] by

$$\varepsilon = \frac{Ntu}{Ntu + 2} \tag{14}$$

where Ntu is the number of transfer units and calculated from

$$Ntu = \frac{4\overline{Nu}L_r}{P_r\overline{R_e}d_h} \tag{15}$$

where $\overline{Nu}, P_r, \overline{R_e}$ and d_h are the average Nusselt number, Prandtl number, average Reynolds number and regenerator hydraulic diameter, respectively. Nusselt number is correlated according to Tanaka as follows

$$\overline{Nu} = 0.33\overline{R_e}^{0.67} \tag{16}$$

The pressure loss due to the gas friction with the regenerator material is calculated from

$$\Delta p_{loss} = -\frac{0.5 f_h \rho L_r U^2{}_{max}}{d_h} \tag{17}$$

where Δp_{loss} is the pressure loss and f_h is the friction factor calculated according to Tanaka from

$$f_h = 1.6 + \frac{175}{Re_{max}} \tag{18}$$

The pressure loss due to the connecting pipe is calculated as

$$\Delta p_{loss} = -\frac{2 f_{Re} \mu L_r U_{av}}{d_h} \tag{19}$$

where f_{Re} is calculated by [34]

$$f_{Re} = \begin{cases} 16 & Re < 2000 \\ 7.343 * 10^{-4} Re^{1.3142} & 2000 < Re < 4000 \\ 0.0791 Re^{0.75} & Re > 4000 \end{cases} \tag{20}$$

The mathematical model is applied to the Karabulut engine at a range of speeds and two pressures. The comparison between the polytropic model and experimental study is shown in Figure 3. The polytropic model has good agreement with the experimental results especially in predicting the trend of engine performance and location of the maximum brake power. The max relative error was calculated as +22% and +30% for the 1 and 2 bar data sets, respectively. Those errors can be attributed to the roughness of the experimental data, lack of data about gas leakage and mechanical friction.

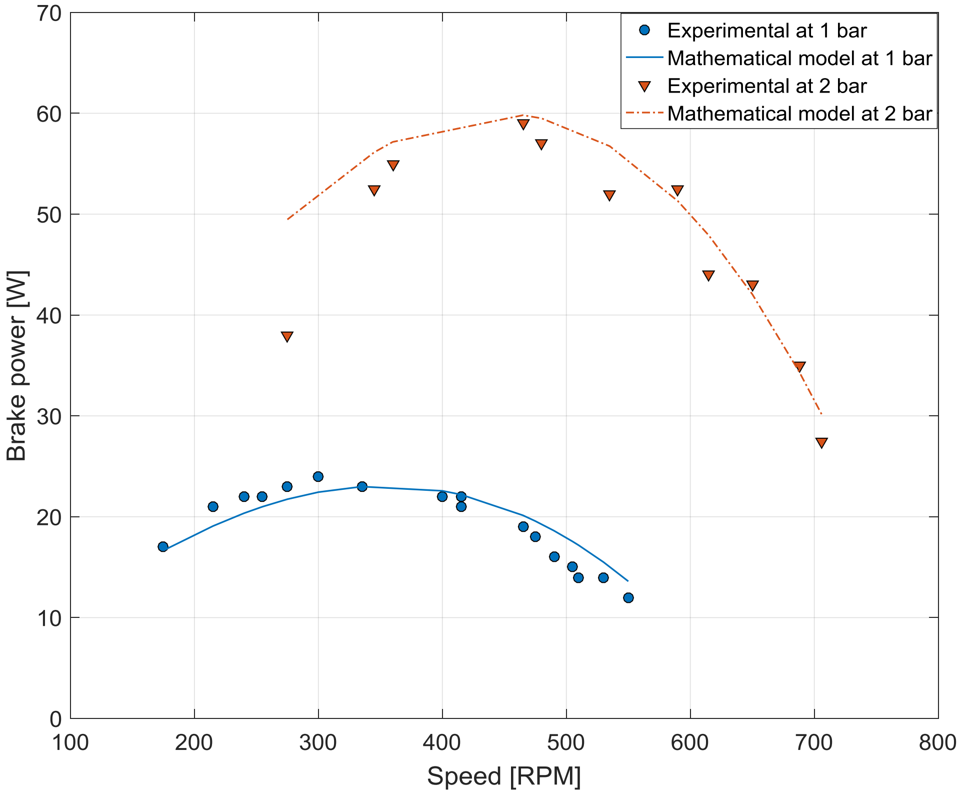

Figure 3: Comparison between the 3 control volume polytropic model with regenerator losses and experimental data of Karabulut alpha type engine [30].

The model is implemented in MATLAB/Simulink and solved using the Runge-Kutta method with a time step of 10^{-4}s. Since the refrigerator has a monotonic response, the parameters are taken from the optimised machine working as a prime mover [27]. The prime mover and the refrigerator have similar phase angle, speed, dead volume, stroke and geometry. All results use the reference machine parameters listed in *Table 2* unless otherwise stated.

Table 2: Parameters of the reference machine

Name	*symbol*	*value/unit*
Stroke length	L_e, L_c	*50 cm*
Bore diameter	D_e, D_c	*5 cm*
Charge gas density	ρ	*1.225 kg/m^3*
Clearance length	re, rc	*0.01 cm*
Regenerator volume	V_r	*0 cm^3*
Out of Phase angle	θ	*90 degree*
Hot, cold temperatures	T_h, T_k	*450K/280 K,300 K*
Working gas	*Air*	
Gas constant	*R*	*287 J/kg.K*

Discussion and Results

The isothermalised Franchot engine has its optimal performance at the maximum power point at which it reaches Curzon efficiency. On the other hand, the cooling power of the Franchot refrigerator depends on the COP. Hence, the performance of the refrigerator is given with reference to the engine. Figure 4 shows the optimised response of the system at the maximum power point for three different design parameters: phase angle for plain cylinder and diameter for both adiabatic and isothermal fin. The optimisation was performed manually until the maximum power is reached for the speed range 100-500rpm. Every single speed, phase angle and connecting rod diameter were changed manually with a step size of 50rpm, 1 degree and 1mm, respectively. The step sizes are believed to be responsible for the roughness in the generated figures.

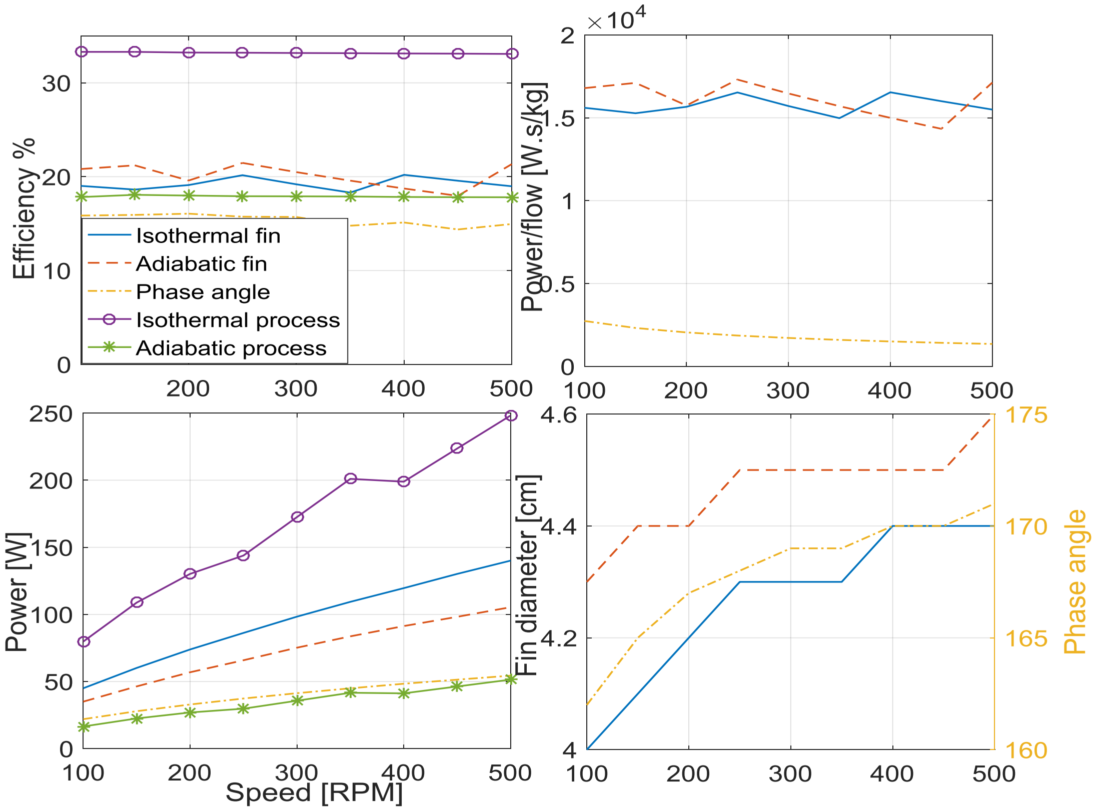

Figure 4: Optimised response based on the maximum power for the Franchot engine using adiabatic and isothermal fins and bare Franchot engine controlled by the phase angle [27].

It is shown that both the isothermal and adiabatic fins are superior to the phase angle control method in terms of power and efficiency. The engine with fins works closer to the Curzon efficiency at the maximum power than the phase angle method. In addition to that, the power obtained is higher for the isothermalised engine than the bare engine optimised by varying the phase angle since the fins increase the heat transfer and heat transfer area. In contrast, the adjustment of the phase angle only optimises the power for a given heat transfer.

It is also shown that optimal cylindrical fin size increases with speed. This is due to the nonlinear increase of the heat transfer in comparison to the swept volume. The fin diameter increases to compensate the increase in the heat required at higher speed by decreasing the hydraulic diameter. It is interesting that the diameter of the isothermal rod is smaller than that of the adiabatic rod, which eases sealing and reduces gas leakage. Most importantly, the bare engine produces much lower power to mass flow rate than the isothermalised engine, which increases regenerator losses. The power to mass flow rate of the isothermalised engine is fixed to a constant value by decreasing the swept volume with increasing speed.

The response of the novel refrigerator is shown in Figure 5 for three different design parameters: phase angle for plain cylinder and diameter for both adiabatic and isothermal fin. The response of the ideal isothermaliser that has ideal expansion and compression processes and the ideal adiabatic engine in which the heaters and coolers are isothermal and the expansion and compression are adiabatic is shown for comparison. Both the ideal isothermal and adiabatic refrigerators have the same swept volume as the isothermal finned design. The isothermal cycle refrigerator presents the maximum possible performance, which gives the Carnot COP.

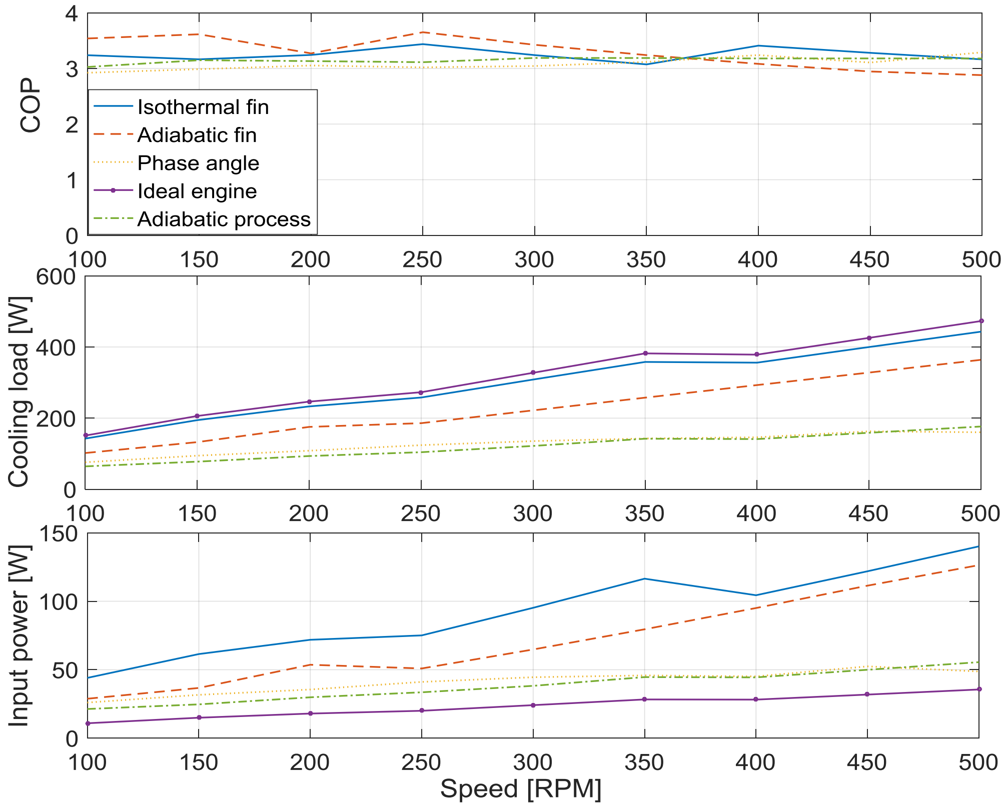

Figure 5: Response of the Franchot cycle refrigerator using adiabatic and isothermal fins and the bare Franchot refrigerator controlled by the phase angle. The response of the ideal refrigerator with isothermal expansion and with adiabatic expansion is shown for comparison.

Finned refrigerators are superior to the phase angle optimised refrigerators as they can achieve higher cooling power at a given efficiency. However, the input power consumed by the refrigerator is higher for the isothermal fin than the bare and adiabatic finned refrigerator. That is expected since the fins increase the heat transfer area and thus the heat transfer.

In comparison to the ideal isothermalisers, which have a COP of 14, the refrigerator with isothermal fins has slightly lower cooling power but has much lower COP. However, the ideal COP is unachievable. In this regard, the ideal adiabatic refrigerator has lower cooling power and efficiency than both the isothermal and adiabatic finned refrigerator at nearly the same COP. On average, the isothermal and adiabatic finned refrigerators have 2.5 and 1.9 times the cooling power of the ideal adiabatic refrigerator at COP of 3.25 and 3.29, respectively. The isothermal and adiabatic finned refrigerator can have an average cooling power of 94% and 72% of the ideal refrigerator. Interestingly, the refrigerators consumed power is comparable to the generated power by the prime mover of the same geometry.

Hence, a duplex engine configuration where the prime mover powers the refrigerator would be suggested for near ambient cooling and medium temperature heat activation.

For near ambient refrigeration, the isothermal finned engine has a COP range comparable to that of the VCC as shown in Figure 6. Thus, the polytropic cycle has greater potential compared to the adiabatic cycle for near ambient cold production. Increasing temperature ratio (ratio of ambient to load temperature) causes the prime mover to speed up hence eventually will reach a steady operation point. On the other hand, decreasing the load temperature increases the required power and hence the engine is anticipated to decelerate. The COP ratio which is the actual COP to Carnot COP reaches zero at load temperature equal to the ambient temperature although the COP is at the maximum. The reason for this is that the gas temperature in the polytropic engine needs to be different from the wall temperature for the heat transfer to take place while the temperature difference in the ideal machine is zero. The improvement in the power density of the polytropic cycle with simple isothermalisers can lead to price reduction and hence can make the Stirling cycle cooler more competitive with the VCC.

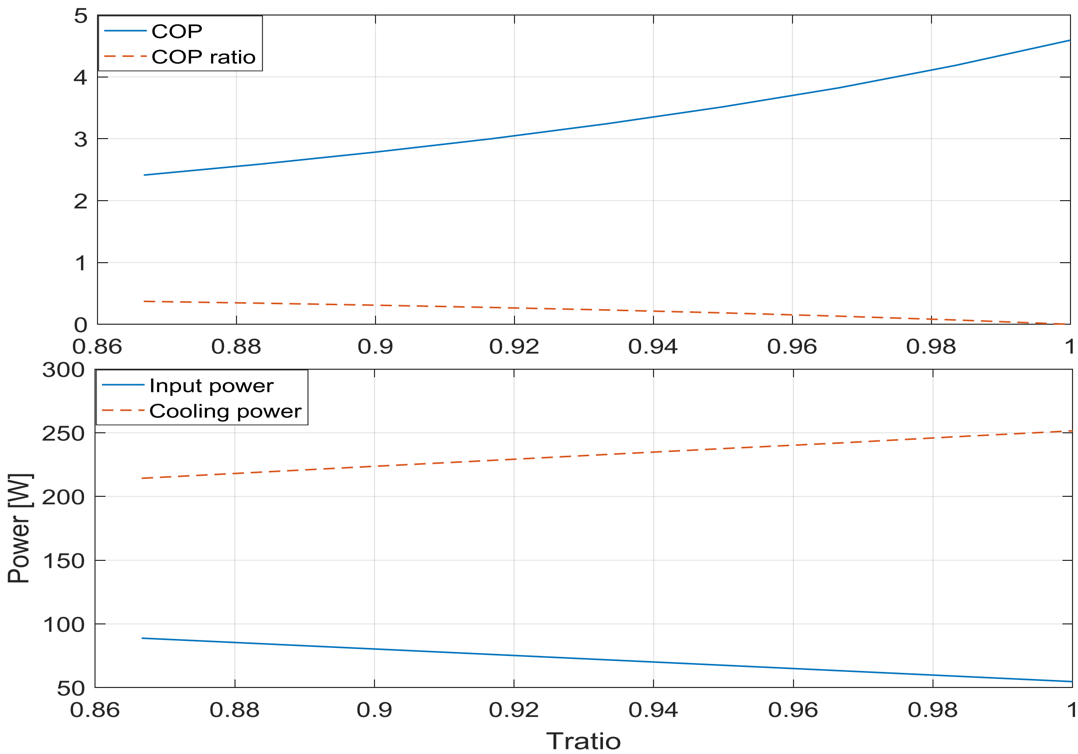

Figure 6: Effect of increasing the temperature ratio of the load to ambient on the COP, COP ratio, input power and cooling power of the isothermal finned cooler at $T_k = 300, n = 200$ rpm and $D_e, D_c = 4.2$ cm.

Conclusion

The machine with isothermalisers resulted in a higher power to mass flow rate in comparison to the bare cylinders for both the engine and refrigerator, which decreases regenerator losses, namely the adiabatic loss that depends on the mass flow rate and the pressure loss that depends on the volumetric flow rate. The simulations show that the Franchot engine can achieve the Curzon efficiency and has the potential to enhance the performance of Stirling engines without using costly and complex heat exchangers. Thus, the performance of the Stirling cycle refrigerators can be improved to be comparable to the conventional VCC in terms of the COP. The isothermalised refrigerator has higher power density than the adiabatic cycle refrigerator. The isothermal and adiabatic fins achieve an average of 2.5 and 1.9 higher power density than the adiabatic engine, respectively.

Larger than 90^o phase angle can be used with some attention to the regenerator losses due to the mass flow rate. However, the finned machine is superior to the adiabatic engine in terms of the power density and hence the regenerator losses.

Acknowledgment

The authors would like to thank Palestine Technical University-Kadoorie (PTUK) for supporting and financing this research paper.

References

[1] M. Gräber and C. Kirches, "Nonlinear model predictive control of a vapor compression cycle based on first principle models," *Proc. 7th Vienna Int. Conf. Math. Model.*, p. 6, 2012.
[2] N. Hariharan and B. P. Rasmussen, "Parameter estimation for dynamic HVAC models with limited sensor information," in *Proceedings of the 2010 American Control Conference*, 2010, pp. 5886–5891.
[3] B. P. Rasmussen and A. G. Alleyne, "Dynamic modeling and advanced control of air conditioning and refrigeration systems," ACRC TR-244, 2006.
[4] L. Bauwens, "Adiabatic Losses in Stirling Refrigerators," *J. Energy Resour. Technol.*, vol. 118, no. June 1996, pp. 120–127, 1996.
[5] H. Hachem, R. Gheith, F. Aloui, and S. Ben Nasrallah, "Optimization of an air-filled beta type stirling refrigerator," *Int. J. Refrig.*, vol. 76, pp. 296–312, 2017.
[6] A. Allouhi, T. Kousksou, A. Jamil, P. Bruel, Y. Mourad, and Y. Zeraouli, "Solar driven cooling systems: An updated review," *Renew. Sustain. Energy Rev.*, vol. 44, pp. 159–181, 2015.
[7] D. Haywood, "Investigation of Stirling-type Heat-pump and Refrigerator Systems Using Air as the Refrigerant," 2004.
[8] G. Walker, G. Reader, R. Fauvel, and E. R. Bingham, "Stirling, Near-Ambient Temperature Refrigerators: Innovative Compact Designs," in *27th Intersociety Energy Conversion Engineering Conference*, 1992, p. 5.93-5.96.
[9] K. Mahkamov, G. Hashem, B. Belgasim, K. Hossin, and I. Mahkamova, "Parametric Analysis of a Dynamic Solar Cooling System Based on a Liquid Piston Converter," *17th Int. Stirling Engine Conf.*, no. December, pp. 59–74, 2016.
[10] D. M. Berchowitz and R. Unger, "Experimental Performance of a Free-Piston Stirling Cycle Cooler for Non-CFC Domestic Refrigeration Applications," in *18th International congress of refrigeration*, 1991.
[11] D. M. Berchowitz, "Stirling Coolers for Solar Refrigerators," in *International appliance technical conference,* 1996.
[12] D. M. Berchowitz, J. Mcentee, and S. Welty, "Design and testing of a 40 W free-piston Stirling cycle cooling unit," in *20th International Congress of Refrigeration*, 1999, no. 1998.
[13] E. Oguz and F. Ozkadi, "Experimental Investigation Of A Stirling Cycle Cooled Domestic Refrigerator," in *International Refrigeration and Air Conditioning Conference*, 2002.
[14] D. G. Thombare and S. K. Verma, "Technological development in the Stirling cycle engines," *Renew. Sustain. Energy Rev.*, vol. 12, no. 1, pp. 1–38, Jan. 2008.
[15] J. D. Van de Ven, "Mobile hydraulic power supply: Liquid piston Stirling engine pump," *Renew. Energy*, vol. 34, no. 11, pp. 2317–2322, 2009.
[16] G. Walker, *Cryocoolers*, Part 1: Fu. Boston, MA: Springer US, 1983.
[17] H. Carlson, M. B. Commisso, and B. Lorentzen, "Maximum Obtainable Efficiency For Engines And Refrigerators Based On The Stirling Cycle," in *Proceedings of the 25th Intersociety Energy Conversion Engineering Conference*, 1990, vol. 5, pp. 366–371.
[18] Anna Helena Orlowska, "An investigation of some heat transfer and gas flow problems relevant to miniature refrigerators," Oxford university, 1985.
[19] F. L. Curzon and B. Ahlborn, "Efficiency of a Carnot engine at maximum power output," *Am. J. Phys.*, vol. 43, no. 1, pp. 22–24, Jan. 1975.
[20] C. H. Blanchard, "Coefficient of performance for finite speed heat pump," *J. Appl. Phys.*, vol. 51, no. 5, p. 2471, 1980.
[21] C. WU, "Maximum Obtainable Specific Cooling Load of a Refrigerator," *Energy Convers.Mgmt*, vol. 36, no. 1, pp. 7–10, 1995.

[22] J. Chen, "Minimum power inputof irreversible Stirling refrigerators for given cooling rate," *Energy Convers. Manag.*, vol. 39, no. 12, pp. 1255–1263, 1998.
[23] H. S. Leff and W. D. Teeters, "EER, COP, and the second law efficiency for air conditioners," *Am. J. Phys.*, vol. 46, no. 1, pp. 19–22, Jan. 1978.
[24] A. Batooei and A. Keshavarz, "A Gamma type Stirling refrigerator optimization: An experimental and analytical investigation," *Int. J. Refrig.*, vol. 91, pp. 89–100, 2018.
[25] J. M. Daoud and D. Friedrich, "Performance investigation of a novel Franchot engine design," *Int. J. Energy Res.*, Aug. 2017.
[26] R. Li and L. Grosu, "Parameter effect analysis for a Stirling cryocooler," *Int. J. Refrig.*, vol. 80, pp. 92–105, Aug. 2017.
[27] J. M. Daoud and D. Friedrich, "Parametric Study of an Air Charged Franchot Engine with Novel Hot and Cold Isothermalizers," *Inventions*, vol. 2, no. 4, p. 35, Dec. 2017.
[28] F. Toda, S. Iwamoto, M. Matsuo, and Y. Umezane, "Heat Transfer on a Small Stirling Engine," *J. Mar. Eng. Soc. JAPAN*, vol. 25, no. 6, pp. 358–365, 1990.
[29] T. S. Zhao and P. Cheng, "Experimental studies on the onset of turbulence and frictional losses in an oscillatory turbulent pipe flow," *International Journal of Heat and Fluid Flow*, vol. 17, no. 4. pp. 356–362, 1996.
[30] H. Karabulut, H. S. YUCESU, and A. Koca, "Manufacturing and testing of a V-type Stirling engine," *Turkish J. Eng. Environ. Sci.*, vol. 24, no. 2, pp. 71–80, 2000.
[31] C. H. Cheng and Y. J. Yu, "Numerical model for predicting thermodynamic cycle and thermal efficiency of a beta-type Stirling engine with rhombic-drive mechanism," *Renew. Energy*, vol. 35, no. 11, pp. 2590–2601, 2010.
[32] B. Kongtragool and S. Wongwises, "Thermodynamic analysis of a Stirling engine including dead volumes of hot space, cold space and regenerator," *Renew. Energy*, vol. 31, no. 3, pp. 345–359, Mar. 2006.
[33] M. Tanaka, I. Yamashita, and F. Chisaka, "Flow and Heat Transfer Characteristics of the Stirling Engine Regenerator in an Oscillating Flow," *JSME Int. J.*, vol. 33, no. 2, pp. 283–289, 1990.
[34] M. Babaelahi and H. Sayyaadi, "Simple-II: A new numerical thermal model for predicting thermal performance of Stirling engines," *Energy*, vol. 69, pp. 873–890, May 2014.